Model predictive-Based direct battery control in PV fed Quasi Z-source inverters

Lashab, Abderezak; Sera, Dezso; Martins, Joäo Pedro Rodrigues; Guerrero, Josep M.

Published in:
2018 5th International Symposium on Environment-Friendly Energies and Applications (EFEA)

DOI (link to publication from Publisher):
10.1109/EFEA.2018.8617084

Publication date:
2018

Document Version
Accepted author manuscript, peer reviewed version

Model predictive-based direct battery control in PV fed Quasi Z-source inverters

Abderezak Lashab, Dezso Sera, João Martins, Josep M. Guerrero
Department of Energy Technology, Aalborg University, Aalborg DK-9220, Denmark
abl@et.aau.dk, des@et.aau.dk, jrm@et.aau.dk, joz@et.aau.dk

***Abstract*—A model predictive-based control strategy for the quasi-Z-source inverter (qZSI) with battery for photovoltaic (PV) power conversion system is proposed in this paper. Usually, in the control of the battery-assisted qZSI, only the injected power to the grid and the maximum power point tracking of the PV are controlled. The battery charges, discharges, or floats depending on the available PV power and demanded power. Thus, a low-frequency current ripple is generated on top of the ripple caused by the shoot through state in the second inductor L_2 and the battery. In the proposed approach, the battery current is directly controlled. The power injection is fulfilled with the maximum power capture from PV panels, along with a decoupled active and reactive power control. The validity of the proposed method is proved by using a detailed simulation model, showing a no low-frequency current ripple in both the inductor L_2 and battery.**

***Keywords*—Feedforward, Grid connected, MPC, MPPT, Three phase, Photovoltaic, P&O, Storage, Z-network.**

I. Introduction

THE growing effort for integration of renewable energy source (RES), is leading to the development of more efficient and compact power electronic converters. One of the most recent trends is the family of impedance-source converters. The voltage fed configurations mainly, Z-source (ZSI) and quasi-Z-source inverters (qZSI) present the advantage of high power density. This is due to the inherent network impedance that allows for a shoot-through state, which boost or buck the output voltage. It is then possible with the same converter configuration to obtain a dc-dc and dc-ac operation [1]. Moreover, the qZSI have other attractive advantages when compared to the ZSI, as it features continuous input current and lower dc voltage on capacitor C_2. In addition, due to the input inductor L_1, the qZSI does not require an input capacitance [2].

One applications where these converters are proving to be successful is for PV applications. In a traditional PV system, a dc-dc converter is first employed in order to match the input voltage of the PV, into the maximum power point (MPP) voltage. This necessarily results in a double stage conversion, in which the impedance-source converters present an advantage. Specifically, the qZSI is capable of extracting a constant current from the PV panels without any extra filtering, and also reducing the switching ripple seen at the PV terminals [3].

Due to the unpredictability as well as the fluctuating solar irradiation, the integration of PV sources presents a challenge for grid operators. In its turn, battery energy storage systems (BESS) have shown the capability of mitigating such a burden [4]. The ability to control and coordinate with PV generation, BESS help to mitigate power fluctuations, maintaining a net power production to the grid. Moreover, BESS can provide ancillary services as frequency regulation, voltage support and supplemental spinning reserve [5].

Traditionally, the integration of BESS in a PV system is possible with a bidirectional dc-dc converter. This converter operates as a charge regulator controlling the charge and discharge rate of the battery. The qZSI allows for the integration of an energy storage without the requirement of additional components. The converter is still capable to regulate the battery state-of-charge (SoC) and at the same time, control the PV output power maximizing the energy production [3]. Two main configurations to integrate the BESS into the qZSI, can be found in the literature. In [6], is proposed to connect the battery directly to capacitor C_2 of the qZSI while in [3] the battery is connected to capacitor C_1. The first configuration has the drawback of a DCM operation when the battery discharges, limiting the inverter output power. The second configuration presents the advantage of a CCM operation during battery discharge but it employs a higher voltage at the battery terminals. As found in the literature, in PV fed qZSI with BESS, a low-frequency current ripple is generated on top of the ripple caused by the shoot through state in the inductor L_2 and the battery as shown in [13], [14], and discussed in [16].

Model-based predictive control (MPC) is gaining increased attention by the research community applied for power electronics. By allowing fast response for multivariable cases, allied with easy integration of nonlinearities and constrains grant this controllers a superior choice [7], [8]. Moreover, when compared with the traditional linear current controls, the MPC does not present the inherent drawbacks of poor performance under grid harmonics, switching dead time and control delay of the common proportional integrators (PI) [7].

The MPC has been proposed for numerous applications in power electronics filed. The four-main categories are grid connected converters, motor drives, inverter with LC filter and inverter with RL load [8]. Moreover, MPC has also been proposed for multilevel inverters, specially: Cascaded H-bridge (CHB) [9], Neutral-point clamped (NPC) converters [10] and

Modular Multilevel Converters (MMC) [11]. MPC has also been proposed for impedance source converters both ZSI and qZSI [12]. All this research demonstrates the increase attractiveness of MPC for power electronics control.

II. Configuration of the Energy Stored Quasi Z-source Inverter

Fig. 1 shows a PV fed three-phase qZSI with the second capacitor C_2 paralleled to a battery. The capacitors C_1 and C_2, the inductors L_1 and L_2, and the diode D are used to form the qZSI network, that is connected to the dc-link of traditional voltage source converter (VSC). In addition to the eight possible switching states of the VSC (seven, considering the two states

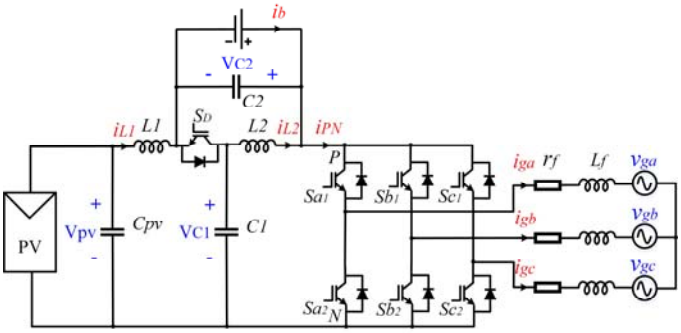

Fig. 1. PV fed Quasi Z-source converter with integrated energy storage.

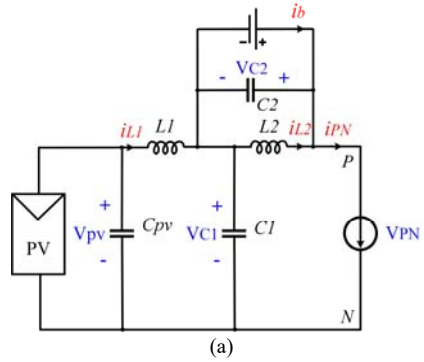

(a)

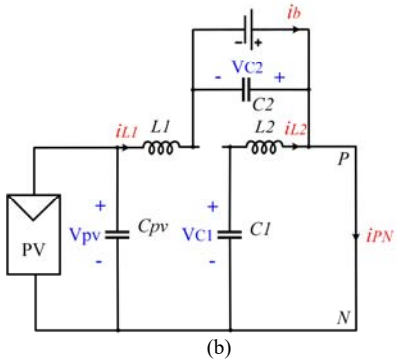

(b)

Fig. 2. PV fed Quasi Z-source converter with integrated energy storage during: (a) active states, and (b) shoot through state.

TABLE I.
Quasi Z-source inverter output Voltage as function of the applied Switching states

	Switching states	Sa_1	Sa_2	Sb_1	Sb_2	Sc_1	Sc_2
ShT state	S_0	*ON*	*ON*	*ON*	*ON*	*ON*	*ON*
	S_1	*OFF*	*ON*	*OFF*	*ON*	*OFF*	*ON*
	S_2	*OFF*	*ON*	*OFF*	*ON*	*ON*	*OFF*
Active states	S_3	*OFF*	*ON*	*ON*	*OFF*	*OFF*	*ON*
	S_4	*OFF*	*ON*	*ON*	*OFF*	*ON*	*OFF*
	S_5	*ON*	*OFF*	*OFF*	*ON*	*OFF*	*ON*
	S_6	*ON*	*OFF*	*OFF*	*ON*	*ON*	*OFF*
	S_7	*ON*	*OFF*	*ON*	*OFF*	*OFF*	*ON*

that provide the same output voltage), a shoot through state (ShT) is also employed to regulate the amplitude of the output voltage as shown in TABLE I. During ShT, all switches of the converter are gated. The equivalent circuits of the qZSI during active states and ShT state are shown in Fig. 2(a) and Fig. 2(b), respectively. The relationship between the output voltage of the Z-network and the ShT duty cycle is given by:

$$\hat{v}_{PN} = \frac{1}{1-2D_{ShT}} v_{pv} \tag{1}$$

such as, D_{ShT} is the ShT duty cycle. The output voltage of the converter as function of the output voltage of the Z-network and the switching states is expressed as:

$$v_{out}(t+T_s) = \frac{2}{3} v_{PN} (S_{a1} + a \cdot S_{b1} + a^2 \cdot S_{c1}) \tag{2}$$

where, $a=e^{-j\frac{2\pi}{3}}$, v_{PN} is the output voltage of the Z-network, v_{out} is the output voltage of the converter, S_{a1}, S_{b1}, and S_{c1} are the switching states of the switches of phase *a*, *b*, and *c*, respectively. By applying Kirchhoff's voltage law on the output side of the converter, the output voltage as function of filter parameters and grid voltage can be found as follows:

$$v_{out} = L_f \frac{di_g}{dt} + r_f i_g + v_g \tag{3}$$

where, i_g is the output current, v_g is the grid voltage, L_f is the output filter inductance, and r_f is the internal resistance of filter inductance. The PV maximum power point tracking is achieved by adjusting the duty cycle of the ShT state, whereas the injected power and the SoC of the battery are controlled through the modulation index (*M*).

III. Proposed Finite-Control-Set MPC for the Energy Stored Quasi Z-source

In FCS-MPC, the first step is the measurement of the controlled variables, in case of qZSI, the capacitor voltage v_{C1}, inductor current i_{L1}, and injected current to the grid i_g. The second step consists of estimating the predicted variables based on the model of the system and the instantaneous measured variables.

In the α,β coordinates, the output voltage can be written as follows:

$$v_{out\{\alpha,\beta\}} = L_f \frac{di_{g\{\alpha,\beta\}}}{dt} + r_f i_{g\{\alpha,\beta\}} + v_{g\{\alpha,\beta\}} \tag{4}$$

Generally, the continuous dynamic equation is converted to a discrete one using Euler's forward approximation:

$$\frac{d\,x(t)}{dt} \approx \frac{x(t+T_s)\text{ - }x(t)}{T_s} \tag{5}$$

where, T_s is the sampling time. By substituting Euler's forward law into (4), we get:

$$i_{g\{\alpha,\beta\}}(t+T_s) = i_{g\{\alpha,\beta\}}(t) + \frac{T_s}{L_f}\Big(v_{out\{\alpha,\beta\}}(t) - r_f i_{g\{\alpha,\beta\}}(t) - v_{g\{\alpha,\beta\}}(t)\Big) \tag{6}$$

such as $i_{out\{\alpha,\beta\}}(t+T_s)$ is the predicted output current for the next sampling time. The first and second terms of the cost function are to fulfil the requirements of the output current, and are given as:

$$g_{\alpha\beta} = \left|i_{g\alpha}^{ref}(t+T_s) - i_{g\alpha}(t+T_s)\right| + \left|i_{g\beta}^{ref}(t+T_s) - i_{g\beta}(t+T_s)\right| \tag{7}$$

In order to control the PV voltage and set it to the voltage that matches the MPP voltage, the converter during active states and during ShT state needs to be considered.

1) During active states:

From Fig. 2(a), and by using Kirchhoff's current and voltage laws, the current through the capacitors and the voltage at the terminals of the inductors can be found as follows:

$$\begin{cases} C_1 \dfrac{dv_{C1}}{dt} = i_{L1} - i_{PN} \\ C_2 \dfrac{dv_{C2}}{dt} = i_{L2} - i_{PN} - i_b \\ L_1 \dfrac{di_{L1}}{dt} = v_{pv} - i_{L1} r_{L1} - v_{C1} \\ L_2 \dfrac{di_{L2}}{dt} = -i_{L2} r_{L2} - v_{C2} \end{cases} \tag{8}$$

Such as v_{C1}, v_{C2}, i_{L1}, i_{L2}, r_{L1}, and r_{L2} are the voltage of capacitor C_1, the voltage of capacitor C_2, the current through inductor L_1, the current through L_2, the stray resistance of the inductor L_1, and the stray resistance of L_2, respectively. By using Euler's law, the capacitor C_1 voltage and inductor L_1 current can be written in discrete time domain form as the following:

$$v_{C1}(t+T_s) = v_{C1}(t) + \frac{T_s}{C_1}\Big(i_{L1}(t) - i_{PN}(t)\Big) \tag{9}$$

$$i_{L1}(t+T_s) = i_{L1}(t) + \frac{T_s}{L_1}\Big(v_{pv}(t) - i_{L1}(t) r_{L1} - v_{C1}(t)\Big) \tag{10}$$

The battery current as function of the inductors current i_{L1},i_{L2} is given by:

$$i_b = i_{L2} - i_{L1} \tag{11}$$

Out of which the battery current in the next sampling instant can be obtained as:

$$i_b(t+T_s) = i_{L2}(t) - \frac{T_s}{L_2} v_{C2} - i_{L1}(t+T_s) \tag{12}$$

2) During shoot through state:

The current through the capacitors and the voltage at the terminals of the inductors during ShT were found similarly as follows:

$$\begin{cases} C_1 \dfrac{dv_{C1}}{dt} = -i_{L2} \\ C_2 \dfrac{dv_{C2}}{dt} = -i_{L1} - i_b \\ L_1 \dfrac{di_{L1}}{dt} = v_{pv} - i_{L1} r_{L1} + v_{C2} \\ L_2 \dfrac{di_{L2}}{dt} = -i_{L2} r_{L2} + v_{C1} \end{cases} \tag{13}$$

From (13), the Z-network variables in the next sampling instant can be written as:

$$v_{C1}(t+T_s) = v_{C1}(t) - \frac{T_s}{C_1} i_{L2}(t) \tag{14}$$

$$i_{L1}(t+T_s) = i_{L1}(t) + \frac{T_s}{L_1}\Big(v_{pv}(t) - i_{L1}(t) r_{L1} + v_{C2}(t)\Big) \tag{15}$$

$$i_b(t+T_s) = i_{L2}(t) + \frac{T_s}{L_2} v_{C1} - i_{L1}(t+T_s) \tag{16}$$

The average value of the current flowing into the capacitor C_{pv} is zero, which implies that the average PV current is equal to the current going through the inductor L_1. Hence, the current of the PV can be regulated at the MPP current using the following cost function:

$$g_L = \left|i_{pv}^{ref}(t+T_s) - i_{L1}(t+T_s)\right| \tag{17}$$

such as $i_{pv}^{*}(t+T_s)$ is the predicted reference PV current, and $i_{L1}(t+T_s)$ is the predicted inductor L_1 current. Since the sampling time T_s is small compared to the sampling time of the references estimation loops, the predicted reference variables can be considered equal to the instantaneous reference variables.

In [13], [14], the battery current is controlled indirectly— the converter injects the amount of demanded power to the grid/load through the modulation index M. Subsequently, the excess of power from the PV goes to the battery, whereas in case of a deficit of power the battery compensates for it. This approach results in low-frequency ripple in both battery and inductor L_2 currents as shown in [13], [14]. Thanks to the multi-objective cost function. In the proposed method, the control of the battery current is also included, in order to eliminate the low frequency current ripple. The fourth term of the cost function is used for controlling the battery current, and is written as:

$$g_b = \left|i_b^{ref}(t+T_s) - i_b(t+T_s)\right| \tag{18}$$

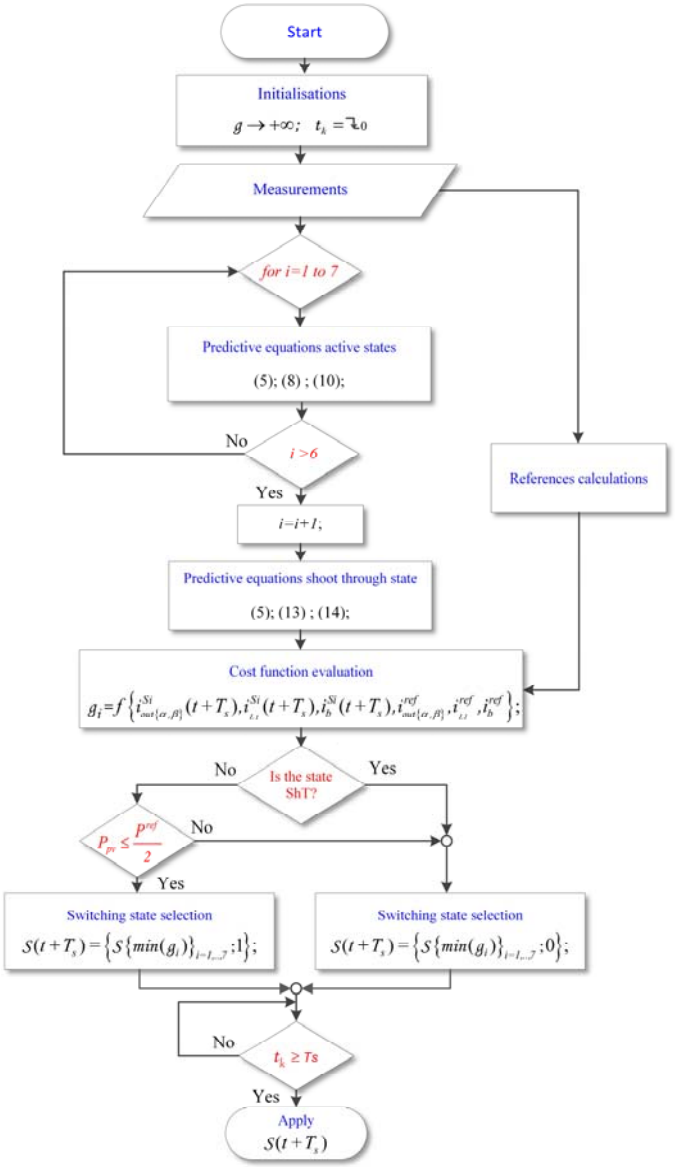

Fig. 3. Flowchart of the proposed MPC for the PV fed qZSI with integrated energy storage.

where $i_b^*(t+T_s)$ is the predicted reference battery current, and $i_b(t+T_s)$ is the predicted battery current. The battery reference current is calculated as:

$$i_b^{ref} = \frac{P_b}{v_{C2}} \tag{19}$$

where P_b, is the power exchanged by the battery. The battery power is defined as the difference between the desired output active power (P^{ref}) and the PV power:

$$P_b = P^{ref} - P_{pv} \tag{20}$$

The third step of FCS-MPC is the cost function evaluation. Contrasted to the control of the qZSI without battery, the voltage of the capacitor C_1 is not controlled here, since its

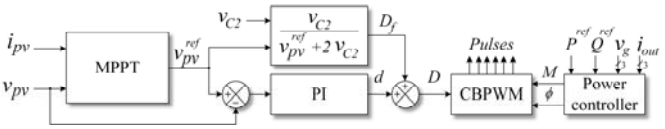

Fig. 4. Control schematic of the PV fed qZI with battery using linear PI controllers.

control may deteriorate the MPP tracking or the battery control or both. In this case, the overall cost function is given by:

$$g = \lambda_{i\alpha\beta} g_{\alpha\beta} + \lambda_{L1} g_{L1} + \lambda_b g_b \tag{21}$$

where, $\lambda_{i\alpha\beta}$, λ_{L1}, and λ_b are the weighting factors of the terms of the output current, the inductor L_1 current and the battery current, respectively. To date, there is no exact method for defining the weighting factors of the cost function [15]. PV fed qZSI with battery suffered from the fact that it can not retrieve from the battery a current higher than the PV current, which implies that the converter can not provide the active desired power when the PV power is less than P^{ref}×50%. Hence, the diode of the Z-network has been replaced by an active switch S_D, which allows a reverse current during low solar irradiance. The switch S_D is triggered ON during all active states of the qZSI in case of low PV power as shown in Fig. 3.

IV. Simulation Results and Discussion

The proposed FCS-MPC for the qZSI with battery has been tested by using a detailed simulation model on MATLAB/Simulink. For comparison purpose, the control of the qZSI with battery by using the linear PI controllers has been also implemented (please see Fig. 4), where Constant Boost PWM (CBPWM) is the chosen modulation strategy. The parameters of the converter are listed in TABLE II. The grid frequency is the same as in Europe, 50Hz. The used PV panels have the following specifications: v_{mp_STC} = 18.5V, I_{mp_STC} = 10.2A, v_{oc_STC} = 22.5V, I_{sc_STC}=16.79A. The PV string is composed of 14 PV panels in series. The MPPT used in this paper is the conventional Perturb&Observe (P&O) with variable step size to speed up the convergence time when changing the solar irradiance level . The used battery is lithium-ion type, and its parameters are shown in TABLE II.

Fig. 5 and Fig. 6 show the simulation results under different solar irradiance levels. From 0s to 1s, the PV generates 2.85kW, from 1s to 2s it generates 2.5kW, and from 2s to 3s it generates 2kW. The demanded active power by the grid is 2.5W.

It can been seen from the results in Fig. 5 and Fig. 6, that during the first level, both the linear PI controllers and the proposed approach are providing a current equal to the desired current, the excess of power is stored in the battery, and the SoC of the battery is increasing. However, it can be seen from these results that when the linear PI controllers are used, a low frequency ripple is present in the inductor L_2 current and subsequently, in the input current I_{PN}, and battery current. In

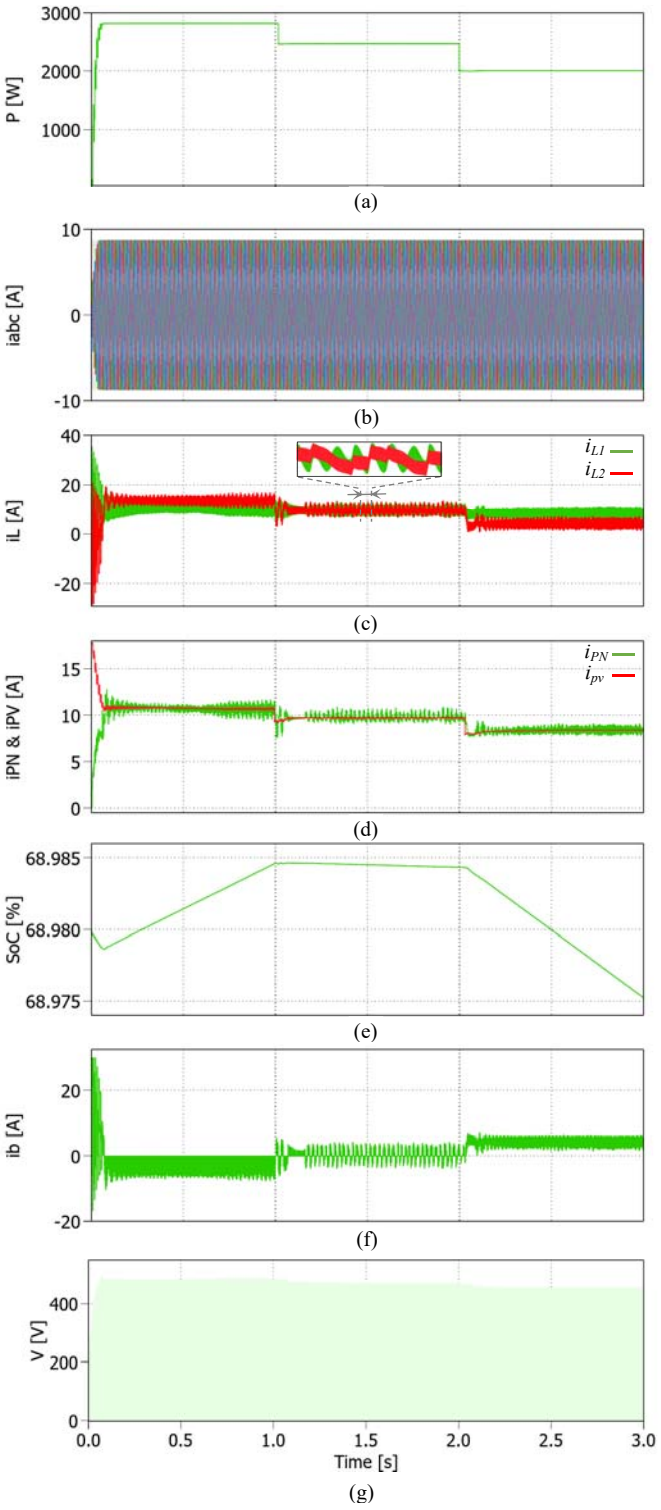

Fig. 5. Simulation results of the battery assisted qZI operating using linear PI controllers under different PV power levels, (a) the drown power from the PV, (b) the output current, (c) the inductor currents of the Z network, (d) the currents of the PV and at the input of the bridge, (e) the SoC of the battery, (f) the battery current, and (g) the voltage at the input of the bridge "v_{PN}".

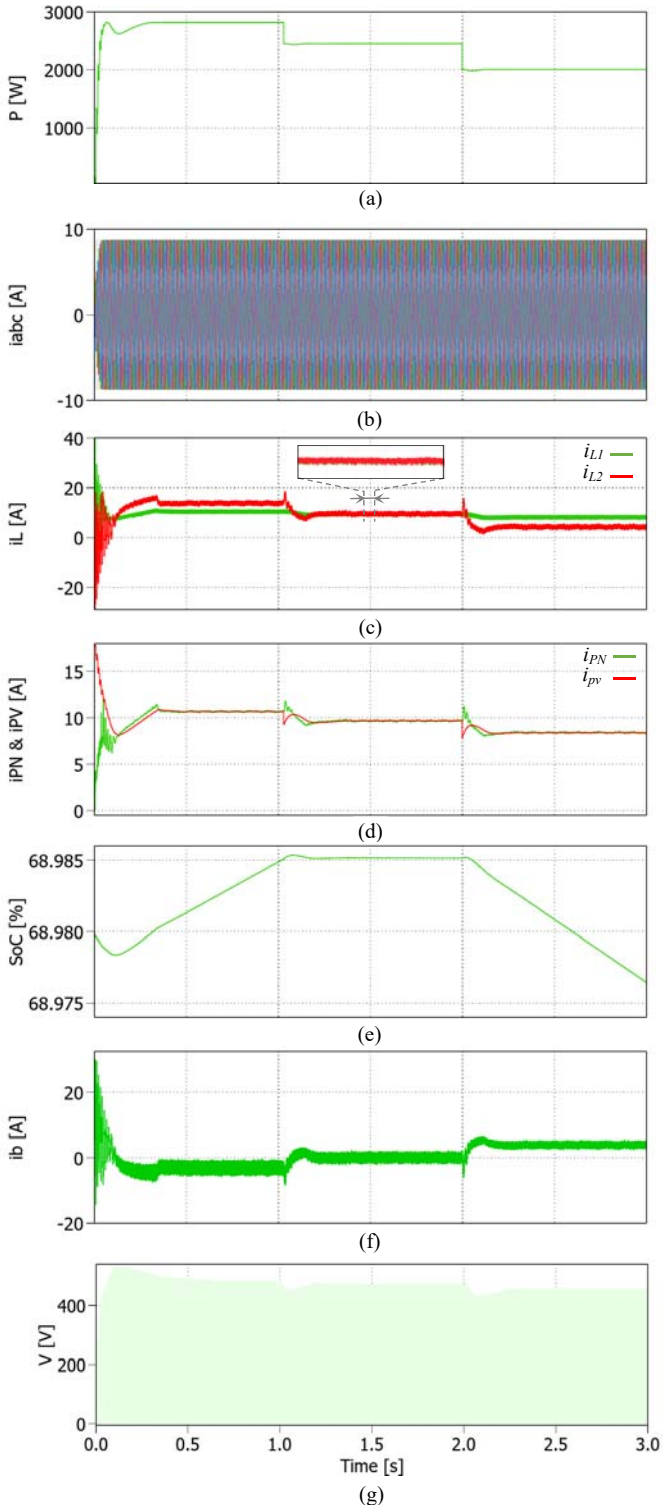

Fig. 6. Simulation results of the battery assisted qZI operating using FCS-MPC under different PV power levels, (a) the drown power from the PV, (b) the output current, (c) the inductor currents of the Z network, (d) the currents of the PV and at the input of the bridge, (e) the SoC of the battery, (f) the battery current, and (g) the voltage at the input of the bridge "v_{PN}".

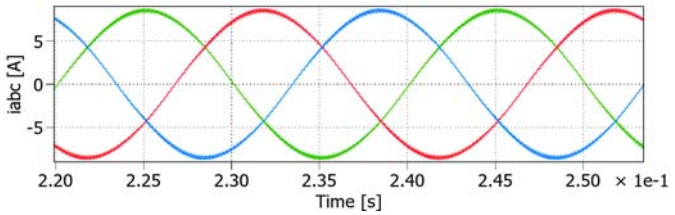

Fig. 7. The current injected to the grid when the systems is operating using linear PI controllers.

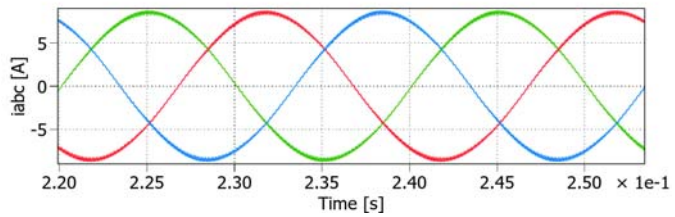

Fig. 8. The current injected to the grid when the systems is operating using FCS-MPC.

TABLE II.
SYSTEM SPECIFICATIONS

Parameter	Value
Filter inductance, Lf	$12mH$
Stray resistor of each inductance, R_L	$0.1Ohm$
Z-network capacitors, $C_{1,2}$	$600\mu F$
PV submodule capacitor, C_{pv}	$1000\mu F$
Switching frequency, f_{sw}	$10KHz$
Battery nominal voltage, $Vbat\_nom$	$100V$
Rated capacity of the battery, Q	$12Ah$

contrast, the proposed approach presents only the high frequency ripple resulted by the ShT state.

One can see from Fig. 5, that the SoC during the first level increased up to 68.9843%, whereas in Fig. 6 the SoC increased up to 68.9852%. Also during the second level, the SoC with the proposed method is fixed to 68.9851%, in contrast, the SoC with the linear controllers is slightly decreasing. It can be concluded that, the SoC is also affected by the ripple of the battery current. Please note that these differences in the SoC are minor, but they are expected to be significant during long time operation.

Fig. 7 and Fig. 8 show the current injected to the grid from the qZSI with the linear PI controllers and proposed method, respectively. As can be seen from these figures, the current with the linear PI controllers has almost the same form compared to FCS-MPC. The reason behind obtaining the same harmonics content is the equivalent switching frequency when using the PI controllers to the sampling time T_s in FCS-MPC.

V. CONCLUSION

A model predictive-based control for PV fed qZSI with battery has been proposed in this paper. The modeling of the power conversion circuit was presented. In contrast to the previously published works, the battery current was directly controlled here. The low frequency ripple in the inductor L_2 current as well as in the battery current were eliminated, while maintaining the high dynamics of the MPP tracking and the injected current to the grid. The simulation results confirmed the effectiveness of the proposed approach in comparison with the linear PI controllers.

VI. REFERENCES

[1] Liu Y, Abu-Rub H, Ge B, Blaabjerg F, Ellabban O, Loh PC. Impedance source power electronic converters. *John Wiley & Sons*; 2016 Oct 3.

[2] J. Anderson and F. Z. Peng, "Four quasi-Z-Source inverters," *PESC Rec. - IEEE Annu. Power Electron. Spec. Conf.*, pp. 2743–2749, 2008.

[3] B. Ge *et al.*, "An energy-stored quasi-Z-source inverter for application to photovoltaic power system," *IEEE Trans. Ind. Electron.*, vol. 60, no. 10, pp. 4468–4481, 2013.

[4] H. Beltran, E. Bilbao, E. Belenguer, I. Etxeberria-Otadui, and P. Rodriguez, "Evaluation of Storage Energy Requirements for Constant Production in PV Power Plants," *IEEE Trans. Ind. Electron.*, vol. 60, no. 3, pp. 1225–1234, 2013.

[5] X. Xu, E. Casale, M. Bishop and D. G. Oikarinen, "Application of new generic models for PV and battery storage in system planning studies," *2017 IEEE Power & Energy Society General Meeting, Chicago, IL*, 2017, pp. 1-5.

[6] J. G. Cintron-Rivera, Y. Li, S. Jiang, and F. Z. Peng, "Quasi-Z-Source inverter with energy storage for Photovoltaic power generation systems," *in 26th proc. IEEE. APEC.* Illinois, pp. 401–406, 2011.

[7] M. Rivera, V. Yaramasu, A. Llor, J. Rodriguez, B. Wu, and M. Fadel, "Digital predictive current control of a three-phase four-leg inverter," *IEEE Trans. Ind. Electron.*, vol. 60, no. 11, pp. 4903–4912, 2013.

[8] S. Vazquez *et al.*, "Model predictive control: A review of its applications in power electronics," *IEEE Ind. Electron. Mag.*, vol. 8, no. 1, pp. 16–31, 2014.

[9] P. Cortes, A. Wilson, S. Kouro, J. Rodriguez, and H. Abu-Rub, "Model predictive control of multilevel cascaded H-bridge inverters," *IEEE Trans. Ind. Electron.*, vol. 57, no. 8, pp. 2691–2699, 2010.

[10] M. Narimani, B. Wu, V. Yaramasu, C. Zhongyuan, and N. Reza Zargari, "Finite Control-Set Model Predictive Control (FCS-MPC) of Nested Neutral Point-Clamped (NNPC) Converter," *IEEE Trans. Power Electron.*, vol. 30, no. 12, pp. 7262–7269, 2015.

[11] B. Riar, T. Geyer, and U. Madawala, "Model Predictive Direct Current Control of Modular Multilevel Converters: Modelling, Analysis and Experimental Evaluation," *IEEE Trans. Power Electron.*, vol. PP, no. 1, pp. 1–1, 2014.

[12] K. Harshath, P. S. Manoharan, and M. Varatharajan, "Model predictive control of Quasi-Z-Source Four-Leg Inverter," *2016 - Bienn. Int. Conf. Power Energy Syst. Towar. Sustain. Energy, PESTSE 2016*, vol. 63, no. 7, pp. 4506–4516, 2016.

[13] H. Abu-Rub, A. Iqbal, S. M. Ahmed, F. Z. Peng, Y. Li, and G. Baoming, "Quasi-Z-source inverter-based photovoltaic generation system with maximum power tracking control using ANFIS," *IEEE Trans. Sustain. Energy*, vol. 4, no. 1, pp. 11–20, 2013.

[14] Dongsen Sun, Baoming Ge, Daqiang Bi, Fang Z. Peng, "Analysis and control of quasi-Z source inverter with battery for grid-connected PV system", *International Journal of Electrical Power & Energy Systems*, vol 46, pp 234-240, 2013.

[15] A. Lashab, D. Sera, J. M. Guerrero, L. Mathe and A. Bouzid, "Discrete Model-Predictive-Control-Based Maximum Power Point Tracking for PV Systems: Overview and Evaluation," *IEEE Trans. Power Electron.*, vol. 33, no. 8, pp. 7273-7287, Aug. 2018.

[16] Y. Liu *et al.*, "Control system design of battery-assisted quasi-z-source inverter for grid-tie photovoltaic power generation," *IEEE Trans. Sustain. Energy*, vol. 4, no. 4, pp. 994–1001, 2013.

[17] H. Snani, M. Amarouayache, A. Bouzid, A. Lashab and H. Bounechba, "A study of dynamic behaviour performance of DC/DC boost converter used in the photovoltaic system," *in 15th proc. IEEE EEEIC*, Rome, 2015, pp. 1966-1971.